



Research article

Impact of anesthetics on rat hippocampus and neocortex: A comprehensive proteomic study based on label-free mass spectrometry

David Astapenko^{a,b}, Marie Vajrychova^{c,*}, Ivo Fabrik^c, Rudolf Kupcik^c,
Kristyna Pimkova^{c,e}, Vojtech Tambor^c, Vera Radochova^d, Vladimir Cerny^{a,f}

^a Department of Anesthesiology and Intensive Care, University Hospital Hradec Kralove, Charles University, Faculty of Medicine in Hradec Kralove, Hradec Kralove, Czech Republic

^b Faculty of Health Sciences, Technical University in Liberec, Liberec, Czech Republic

^c Biomedical Research Center, University Hospital Hradec Kralove, Hradec Kralove, Czech Republic

^d Vivarium Department, Faculty of Military Health Sciences, University of Defence, Brno, Czech Republic

^e Biocev, 1st Faculty of Medicine, Charles University in Prague, Czech Republic

^f Dept. of Anesthesiology, Perioperative Medicine and Intensive Care, Hospital Bory, Bratislava, Slovak Republic

ARTICLE INFO

Keywords:

Label-free proteomics
Anesthetics
Neocortex
Hippocampus
Long-term potentiation
NMDAR
GABA signaling
VDAC
Apoptosis

ABSTRACT

Anesthesia is regarded as an important milestone in medicine. However, the negative effect on memory and learning has been observed. In addition, the impact of anesthetics on postoperative cognitive functions is still discussed. In this work, *in vivo* experiment simulating a general anesthesia and ICU sedation was designed to assess the impact of two intravenous (midazolam, dexmedetomidine) and two inhalational (isoflurane, desflurane) agents on neuronal centers for cognition (neocortex), learning, and memory (hippocampus). More than 3600 proteins were quantified across both neocortex and hippocampus. Proteomic study revealed relatively mild effects of anesthetics, nevertheless, protein dysregulation uncovered possible different effect of isoflurane (and midazolam) compared to desflurane (and dexmedetomidine) to neocortical and hippocampal proteins. Isoflurane induced the upregulation of hippocampal NMDAR and other proteins of postsynaptic density and downregulation of GABA signaling, whereas desflurane and dexmedetomidine rather targeted mitochondrial VDAC isoforms and protein regulating apoptotic activity.

1. Introduction

Neurotoxicity induced by general anesthetics may be detrimental for both developing [1,2] and aging brain [3,4]. It has been suggested that both inhalational and intravenous anesthetics may evoke the morphological and biochemical neuronal changes resulting in neuronal cell death [5]. Moreover, there is alarming evidence about the postoperative delirium (POD) and postoperative cognitive dysfunction (POCD) developed after exposure to anesthetics in long-term neurodevelopmental delay [6,7]. Despite undisputed benefit of anesthetics in medicine, it is necessary to highlight the mechanism leading to neuroapoptosis and long-lasting impairment of cognitive function. On the other hand, the neuroprotective role of both intravenous and volatile anesthetics is also

* Corresponding author. Biomedical Research Center, University Hospital Hradec Kralove, Sokolska 581, 500 05, Hradec Kralove, Czech Republic.
E-mail address: marie.vajrychova@fnhk.cz (M. Vajrychova).

<https://doi.org/10.1016/j.heliyon.2024.e27638>

Received 18 September 2023; Received in revised form 4 March 2024; Accepted 4 March 2024

Available online 5 March 2024

2405-8440/© 2024 The Authors. Published by Elsevier Ltd. This is an open access article under the CC BY-NC-ND license (<http://creativecommons.org/licenses/by-nc-nd/4.0/>).

discussed. There is growing number of studies with animal models focused on dexmedetomidine as neuroprotection against various insults in the brain like focal cerebral ischemia [8,9]. A partial neuroprotective effect of volatile desflurane, sevoflurane and isoflurane was found in case of neonatal hypoxia/ischemia reperfusion [10].

Currently, midazolam and dexmedetomidine are used intravenously to induce very fast sedation of intensive care unit's patients (ICU). Midazolam (MID) represents short-acting benzodiazepine used particularly for procedural sedation, e.g. during gastrointestinal endoscopy. This agonist of γ -aminobutyric acid (GABA) receptor has been studied for more than fifty years especially due to the development of neuroimaging field. Beside its sedative, amnesic, anxiolytic, hypnotic and myorelaxant effect it may cause confusion, delirium, oversedation and respiratory depression [11]. In addition, based on its pharmacokinetics, it is prone to cumulation and unpredictable recovery upon withdrawal in ICU patients [12]. Dexmedetomidine (DEX) is a highly selective α_2 adrenoceptor agonist approved for use as an adjunct agent for sedation and analgesia in ICU [13,14]. It has been shown that the DEX – induced sedation is the most similar to a physiological sleep and it is one of the most effective treatment for POD [15]. Although application of DEX may produce hypotension and bradycardia, its impact on the brain integrity is less pronounced compared to other sedative agents [16]. Beside the animal model, the neuroprotective effect of DEX has been shown also in the human [17,18].

Isoflurane and desflurane are volatile anesthetic agents used commonly to maintain GA. Isoflurane (ISO, 1-chloro-2,2,2-trifluoroethyl difluoromethyl ether) has been widely induced as a cost-effective anesthetic for the last 40 years [19]. However, its neurotoxicity has been proven on rodent models [20–22]. Also, there was established a link to the POCD development in humans [1,23,24] and isoflurane is currently no longer registered for clinical use in some countries. The chemical structure of desflurane (DES, 1,2,2,2-tetrafluoroethyl difluoromethyl ether) is similar to ISO, but chlorine atom is substituted by fluorine atom on the α -ethyl carbon. Due to complete fluorination, DES is less metabolized and less prone to defluorination than isoflurane and other inhalational anesthetics (methoxyflurane, enflurane, and sevoflurane) [25]. DES acts on the same receptors as isoflurane: agonist on GABA- α complex and glycine receptors, antagonist on nicotinic receptors and ligand-gated ion channels [26,27]. Due to its lower potency it is better titratable and recovery from anesthesia is faster and more predictable. Desflurane was expected to be less neurotoxic [28], although studies in recent years are mostly inconclusive in terms of preference of one potentially less harmful agent [29,30].

Current research and development in neurology is focused on the anesthetic agents with less neurotoxic effect on the human brain [31]. Also, the type of anesthetics represents a clinical dilemma as it has been demonstrated in comparison of total intravenous anesthesia with propofol and inhaled anesthetics [32]. In this work, we stepped on the assessment of anesthetic impact based on comparison of protein levels. Quantitative proteomic analysis based on mass spectrometry has currently stable and unflappable position in the basic research and human brain proteome is in the front of scientific interest. This fact was recently supported by the formation of Human Brain Proteome Project (www.hbpp.org), a new initiative with the aim of unveiling the brain proteome. The large-scale proteomic studies serve as valuable tools to map biochemical processes and signaling pathways associated with pathological brain alteration (e.g. neurodegenerative diseases [33]). Similar to neurodegeneration, a global proteomic study may identify proteins reflecting the impact of anesthetic agents in point of e.g. neurotoxicity and neuroapoptosis. We therefore aimed to study proteome of the rat hippocampus and the frontal lobe treated by two inhaled anesthetics, isoflurane and desflurane, and two intravenous sedatives, midazolam and dexmedetomidine to induce 5 h lasting anesthesia/sedation.

2. Materials and methods

2.1. Reagents and chemicals

This study did not generate new unique reagents. All reagents and chemicals for tissue homogenization following by protein digestion were purchased from Sigma Aldrich (St. Louis, MO, USA), if not specified otherwise. Organic solvents and water (LC-MS grade) were purchased from Honeywell (Morris Plains, NJ, USA). All reagents for SDS-PAGE and immunoblotting were purchased from Invitrogen (Carlsbad, CA, USA) and Thermo Fisher Scientific (Waltham, MA, USA).

2.2. Data and code availability

The mass spectrometry data together with the MaxQuant output files have been deposited in the ProteomeXchange Consortium via the PRIDE partner repository [34] with the dataset identifier PXD045159 and are publicly available as of the date of publication.

2.3. Ethical committee approval

The experimental study was approved by the Animal Welfare Committee of the University of Defence, Faculty of Military Health Sciences in Hradec Kralove, Czech Republic (approval no. 17–20/2014-6848) in accordance with Czech legislation on the protection of animals that complies with the Directive 2010/63/EU of the European Parliament and Council.

2.4. Design of the experimental groups

Ten rats (*Rattus norvegicus*, Velaz, Prague, Czech Republic); 5 males, 5 females equally divided into groups) were chosen to conduct the study. The animals were provided with tap water and rodent laboratory chow (Velaz, Prague, Czech Republic) *ad libitum* under standard 12 h light/dark rhythmic conditions. Animals were split into 3 groups: 4 rats in intravenous (i.v.) anesthesia group (IV group) – 2 to be anesthetized/sedated with midazolam and 2 with dexmedetomidine; 4 rats in inhalational anesthesia group (INH group) – 2 to

be anesthetized with isoflurane and 2 with desflurane; and 2 rats in control group. Intraperitoneal (i.p.) induction was performed after prior sedation with halothane (Narkotan, Zentiva, Prague, Czech Republic) until the animals fall asleep in closed box. Ketamine was injected i.p. in a dose 75 mg/kg (Narkamon, 10%, Spofa, Czech Republic) with xylazine 2 mg/kg (Xylazine, 2%, Oostkamp, Belgium). After induction the inguinal area on both sides was shaved for cannulation of vasa femoralia. Arteria femoralis with 24G catheter for invasive blood pressure monitoring and vena femoralis for infusion of crystalloid solution in dose 10 mL/kg per hour (Ringerfundin, B Braun, Melsungen, Germany). Catecholamines were not used during the experiment.

2.5. Application of the anesthetics

Two animals in INH group were placed into the hermetic box connected to the anesthesia machine (Datex-Ohmeda GE Healthcare, Cirrus Anesthesia Machine) with interior concentration of isoflurane (Forane, Abbott, Chicago, Illinois, USA) 1 % in mixture of oxygen ($F_{I}O_2 = 0.4$) and air breathing spontaneously. Two animals received desflurane (Suprane, Baxter, Lessines, Belgium) 6 % in mixture of oxygen ($F_{I}O_2 = 0.4$) and air breathing spontaneously. The animals were left inside for 5 h (h) and 10 min. Temperature was kept on 37 °C with heating pad (Heating desk VD type 1, Vitrum Praha Ltd, Praha, Czech Republic) inserted at the bottom of the box and measured with rectal probe.

Two animals in IV group were connected to the linear dosing machine (B Braun, Melsungen, Germany) to be administered midazolam (Midazolam, Accord Healthcare Limited, Middlesex, UK) in a rate of 0.85 mg/kg per hour i.v. Two animals were given dexmedetomidine (Dexdor, Orion Pharma, Espoo, Finland) in a rate of 1 µg/kg per hour i.v. The IV animals were also placed on the heating pad and the rectal temperature was measured leaving the animal to ventilate spontaneously. The tube with fresh gas mixture ($F_{I}O_2 = 0.4 + \text{air}$) was placed near the nostrils. The animals were kept in this setting for 5 h and 10 min. During anesthesia the following vital signs of both groups (IV + INH) were continuously monitored and recorded every 10th minute; invasive blood pressure (mean arterial blood pressure), heart rate, blood oxygen saturation, respiratory rate and rectal temperature (monitor GE Datex Ohmeda S5 Compact Monitor, Hoyer, Prague, Czech Republic). Subsequently, an adequate level of anesthesia was assessed based on corneal reflex, nociceptive reflex, and movement.

2.6. Tissue collection and homogenization

All animals were exsanguinated and perfused with normal saline (F1/1, B Braun, Melsungen, Germany) for maximal preservation of brain tissue and maximal erythrocyte washout off the capillaries at the end of the experiment. Needle (18 G) was inserted into the left ventricle after midline thoracotomy and prior deepening of anesthesia with ketamine (1 mg/kg i.v.). The right atrium was punctured and the infusion with normal saline was turned on until the exsanguination and asystole occurred. The brain of the animal was then withdrawn after craniotomy and the sites of our interest (neocortex and hippocampus) were isolated, weighted and frozen with liquid nitrogen. The time of brain tissue ischemia was noted as time interval from the asystole to the freezing of the samples. The right hemisphere neocortex and hippocampus were frozen at – 80 °C and 3% sodium deoxycholate (SDC) was added in 1:4 ratio (mg of brain structure: µl of SDC). Brain structures were homogenized by bench dispersing instrument (T 10 basic ULTRA-TURRAX, IKA®-Werke GmbH & Co. KG, Staufen, Germany) at 8000 rpm for 1 min. Subsequently, samples were heated to 40 °C for 45 min under continuous shaking (1000 rpm), centrifuged at 10 000 rpm (10 min, 4 °C) and supernatant was kept for further analysis at – 80 °C. Total protein concentration was determined by bicinchoninic acid and copper sulfate solutions (BCA protein assay kit).

2.7. Protein digestion

From each homogenized sample, a 20 µg was taken for protein digestion. SDC was added to a final concentration of 1 % for enhancement of digestion efficiency. The pH was adjusted by 1 M triethylammonium bicarbonate buffer (TEAB, Thermo Scientific, Rockford, IL, USA) to final concentration of 100 mM TEAB. Disulphide bonds were reduced by 5 mM tris(2-carboxyethyl) phosphine hydrochloride (TCEP) for 1 h at 60 °C, and free thiol groups were blocked using 10 mM methyl methanethiosulfonate (MMTS) for 30 min at room temperature under continuous shaking (950 rpm). Proteins were digested using rLys-C (Wako Pure Chemical Industries, Osaka, Japan) for 4 h at 37 °C followed by sequencing grade trypsin (Promega, Madison, WI, USA) digestion at 37 °C overnight. Both proteases were added at a 1:50 enzyme to protein ratio (w/w).

2.8. Sodium deoxycholate extraction and peptide desalting

All samples were acidified by trifluoroacetic acid (TFA) to a final concentration of 1 % to stop protease digestion. Sodium deoxycholate was removed from all samples using extraction in water-saturated ethyl acetate (EA). Briefly, all samples were shaken with 300 µl of EA followed by centrifugation at 10 000 rpm for 45 s. The organic phase was discarded and the whole procedure was repeated three times. The remaining EA traces in the aqueous phase were evaporated and 0.1% TFA in 5% acetonitrile (AcN) was added into a final volume of 0.5 mL. Subsequently, samples were centrifuged at 10 000 rpm for 2 min and the supernatants were loaded onto C18 phase of Empore C18-SD SPE cartridges (3 M, St. Paul, MN, USA), previously washed using 1 mL of methanol and equilibrated using 0.1% TFA in 5% AcN. After supernatant loading, C18 phase was washed twice using 1 mL of 0.1% TFA in 5% AcN and trapped peptides were released in 300 µl of 0.05% TFA in 50% ACN. Finally, all samples were evaporated into the dryness.

2.9. Liquid chromatography coupled to mass spectrometry analysis (LC-MS)

Samples were re-dissolved in 0.1% TFA in 2% AcN to a concentration 1 µg/µl and 3 µg were injected in three technical replicates. Chromatographic separation of peptides was conducted on UltiMate 3000 RSLCnano system (Thermo Scientific, Bremen, Germany). The analytical system consisted of PepMap100C18, 3 µm, 100 Å, 75 µm × 20 mm trap column and PepMap RSLC C18, 2 µm, 100 Å, 75 µm × 500 mm analytical column (both from Thermo Scientific). The samples were loaded onto the trap column in 0.1% TFA in 2% AcN at 8 µl/min for 3 min. Tryptic peptides were separated using segment linear gradient running from 2% to 9%, then 34.5% and 45% of 80% AcN with 0.1% FA for 57 min, 160 min and 23 min at a flow rate of 200 nL/min; respectively. Eluted peptides were electrosprayed into Q-Exactive Plus using a Nanospray Flex ion source (Thermo Scientific, Bremen, Germany). Positive ion full scan MS spectra were acquired in the range of 350–1600 *m/z* using 3×10^6 AGC target in the Orbitrap at 70 000 resolution with a maximum ion time of 100 ms. For fragmentation, the MS/MS spectra were acquired for 10 most intensive precursors. The isolation window was set to 2.0 *m/z* and normalized collision energy (NCE) was set up 28%. Precursor ions charge state was set to ≥ 2 . Dynamic exclusion window of 19.0 s was selected for HCD fragmentation. MS/MS spectra were acquired at resolution of 17 500, with a 1×10^5 AGC target and a maximum injection time of 60 ms.

2.10. Mass spectrometry data processing and evaluation

Acquired RAW files were processed by MaxQuant ver. 1.6.3.4 [35]. Data were searched against FASTA database of reference proteome for *Rattus norvegicus* downloaded from Uniprot (January 4, 2019) including potential contaminants. Protein identification was performed using subsequent parameters: mass tolerance for the first search 20 ppm, for the second search from recalibrated spectra 4.5 ppm (with individual mass error filtering enabled); maximum of 2 missed cleavages; maximal charge per peptide $z = 7$; minimal length of peptide 7 amino acids, maximal mass of peptide 4600 Da; cysteine S-methylthiolation as fixed and protein acetylation on N-term and methionine oxidation as variable modifications with the maximum number of variable modifications per peptide set to 5. Trypsin with no cleavage restriction was set as a protease. Mass tolerance for fragments in MS/MS was 20 ppm, taking the 12 most intensive peaks per 100 Da for search (with enabled possibility of cofragmented peptide identification). Minimal Andromeda score for modified peptides was 40, minimal delta score for modified peptides was 6, and FDR filtering on peptide spectrum match and protein level were both set to 0.01. All hits identified in searches as contaminants were filtered out. Proteins were quantified using MaxLFQ [36] with at least 2 peptide ratios required for pair-wise comparisons of protein abundance between samples. MaxLFQ intensities for each protein per biological replicate were averaged from at least two technical replicates (i.e. injections/measurements). Only those proteins having coefficient of variance <25% between biological replicates ($n = 2$) were kept and their MaxLFQ intensities were averaged to obtain final protein abundance per experimental sample group. Protein abundances from treated groups were divided by the values from control groups of the respective tissue and the resulting ratios were log2-transformed. Proteins significantly regulated by used anesthetics were found by Significance B function implemented in Perseus software [37]. MaxLFQ values summed from both treated and control groups per each protein were used as intensity columns and Benjamini-Hochberg FDR 0.05 was used as cut off value. All bar graphs were designed in GraphPad Prism 6. Scatter plots, heatmaps and PCA plots were designed in R statistical environment.

2.11. SDS-PAGE and immunoblotting

SDS-PAGE and immunoblotting were performed according to the standard protocols for NuPAGE electrophoresis and semi-dry Western blot provided by producer. 20 µg of neocortex and hippocampus homogenized samples pooled from replicates for the

Table 1

Basal vital signs of animals included in this study. One male and one female rat was used in each control and anesthetics group. The two intravenous anesthetics (midazolam and dexmedetomidine) and two inhalational agents (isoflurane and desflurane) were applied. The basal values of mean arterial pressure, heart rate, blood oxygen saturation, respiration rate and rectal temperature were determined in case of each animal along with the weight and time of ischemia.

Group	Control		Intravenous (IV)				Inhaling (INH)			
			MID		DEX		ISO		DES	
Anesthetic	–		MID		DEX		ISO		DES	
ID of animal	A	B	A	B	A	B	A	B	A	B
Weight [g]	416	391	423	501	421	458	386	540	648	481
Time of ischemia [min]	16.30	15.83	12.37	13.83	15.00	16.53	17.58	13.53	14.38	18.50
Basal values	Control		MID		DEX		ISO		DES	
MAP [mmHg]	90	90	90	102	105	120	85	140	126	95
HR [beats/min]	230	250	190	240	255	242	255	250	280	260
SpO ₂ [%]	98	96	99	96	96	90	98	95	98	96
RR [breaths/min]	62	63	60	65	60	60	65	65	60	55
Temp [°C]	36.9	36.5	36.5	36.5	36.5	36.4	36.2	36.2	36.5	36.6

Abbreviations: MAP–mean arterial blood pressure, HR–heart rate, SpO₂–blood oxygen saturation, RR–respiratory rate, Temp–rectal temperature, MID–midazolam, DEX–dexmedetomidine, ISO–isoflurane, DES–desflurane.

given treatment in reducing LDS sample buffer were separated by SDS-PAGE on a gradient gel (4–12%) and detected by western blotting. PVDF 0.45 μm membranes were blocked for 30 min in 10% milk at room temperature, incubated with primary antibodies overnight at 4 °C and after washing with TBS/Tween-20, incubated with appropriate secondary antibody for 1 h at room temperature. All antibodies used in this study were summed in [Supplementary Table S1](#) (see Supplementary document). Proteins were visualized using chemiluminescence (Amersham ECL reagents, Thermo Fisher Scientific) using Azure c280 (Azure Biosystems, Dublin, CA, USA). Original pictures of immunoblotting membranes were summed in the Supplementary Document.

3. Results and discussion

3.1. Vital signs of animals during sedation/anesthesia simulation

In this work, we exploited label-free LC-MS/MS analysis to analyze proteome changes induced by two inhalational (ISO, DES) and intravenous (MID, DEX) anesthetics in rat neocortex and hippocampus, fundamental brain structures for cognitive function (neocortex), learning, and memory (hippocampus). Experiment mapping the short-term impact of anesthesia without surgical stimulation was designed and four anesthetics drugs were investigated to examine if even a few hours of administration carry the potential to induce the shift of protein levels in neocortex and hippocampus. Basal values of animals before the application of anesthetics were listed in [Table 1](#). DEX induced a permanent decrease of mean arterial pressure ([Supplementary Fig. 1A](#)) along with continuous increase of heart rate ([Supplementary Fig. 1B](#)). We presume, that blood pressure instability may have occurred, since DEX is not used for the maintenance of general anesthesia. The monitored values of oxygen saturation (SpO₂) and respiratory rate (RR) showed similar trends observed in commonly conducted anesthesia in medical practice ([Supplementary Fig. 1C and D](#)).

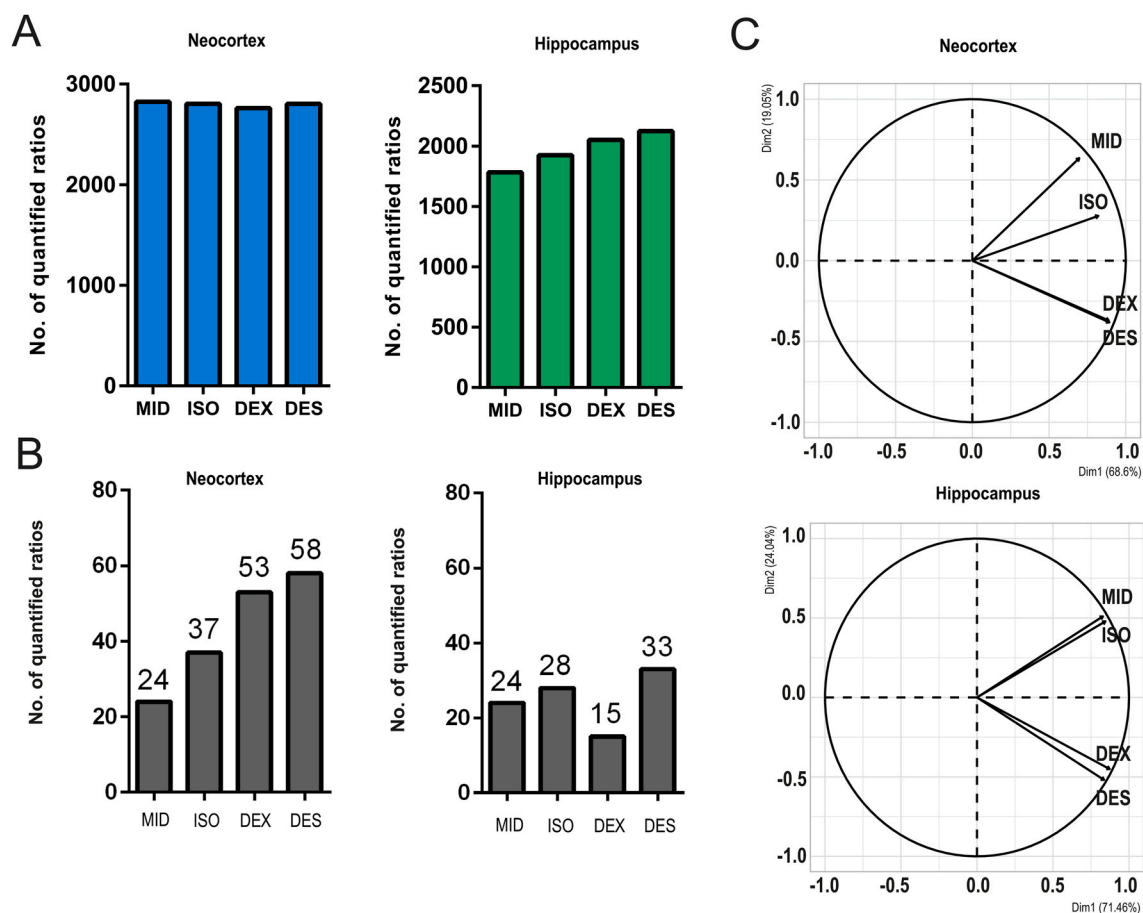


Fig. 1. Yield of comparative label-free proteomic study. (A) Number of all quantified proteins with variability under 25% between biological replicates. (B) Number of significantly changed proteins in neocortex and hippocampus. (C) PCA plots illustrating the proximity of anesthetics based on protein dysregulation in neocortex and hippocampus.

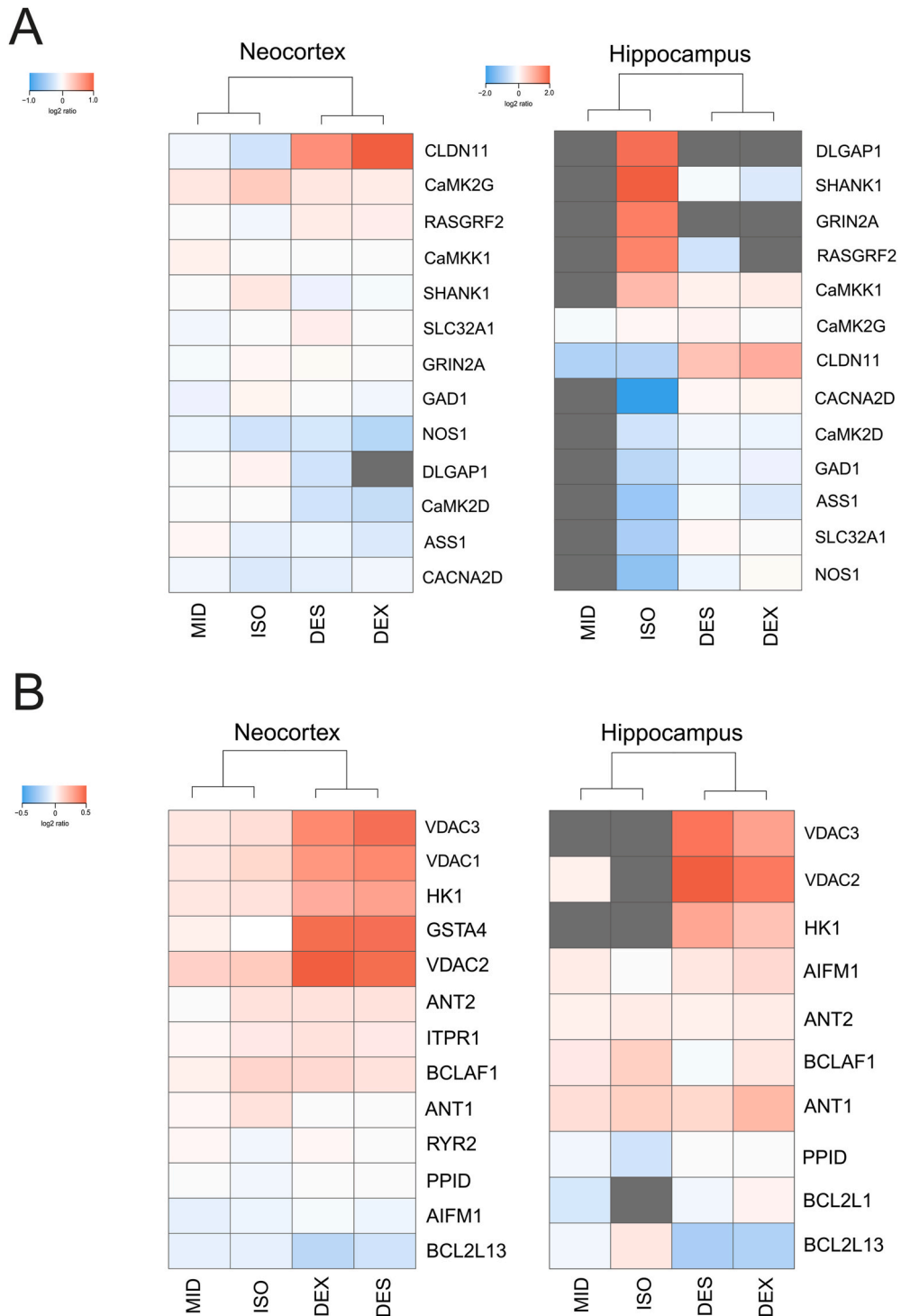


Fig. 2. Change of proteins related to applied anesthetic/sedation agents. (A) Heatmaps illustrating the relative level of proteins induced by anesthetics. Proteins related to long-term potentiation pathway were included into the clustering. Missing values are depicted in grey in the heatmaps. (B) Heatmaps illustrating the relative level of proteins induced by anesthetics. Proteins related to mitochondrial-mediated apoptosis were included into the clustering. Missing values are depicted in grey in the heatmaps.

3.2. Mild effect of sedation/anesthesia to global proteomes, but still different between isoflurane and desflurane

After the 5 h, the simulation of anesthesia/sedation was ended, rats were sacrificed and brain tissues were processed for LC-MS/MS as described in Method details. Conducted LC-MS/MS analysis yielded in total 3603 quantified proteins with protein level variability below 25 % between two biological replicates. On average, 2931 neocortical proteins and 2231 hippocampal proteins were quantified across all investigated anesthetics if at least 1 valid value was required (Fig. 1A, Supplementary Table S2). Global effect of anesthetics on brain proteome was relatively mild as only minority part of neocortical (24–58) and hippocampal (15–33) proteins were confirmed as significant outliers (Fig. 1B, Supplementary Table S2). However, we observed similar impact to proteins of DES and DEX compared to ISO along with MID (Fig. 1C).

3.3. Impact of isoflurane to hippocampal postsynaptic long-term potentiation

Despite similar chemical structures of ISO and DES and shared protein target, our data suggests different effect to specific neocortical and hippocampal proteins especially related to postsynaptic long-term potentiation (LTP) (Fig. 2A) and mitochondria-induced apoptosis (Fig. 2B). We therefore discuss our results considering especially these two pathways as closely connected with neurodegenerative process. Changes of synaptic plasticity are widely considered as a principal mechanism of memory storage [38]. Involving calcium signaling. In neurons, the elevation of cytosolic calcium is realized through influx of extracellular calcium by opening NMDAR and voltage-gated calcium channels or through calcium efflux from endoplasmic reticulum via ITP and RYR receptors. Calcium/calmodulin-regulated protein kinases (CaMK) are involved in kinase-dependent signaling coupling to NMDAR and leading to induction of LTP. Perturbations in calcium homeostasis may result in disorders like Alzheimer's and Parkinson's, since synaptic loss and dysfunction belong to the early signs of neurodegenerative process. On the other hand, brain is metabolically active organ containing large number of mitochondria [39] and abnormal cytosolic calcium influx into mitochondria might result in neuronal apoptosis [40–42].

Specifically, in hippocampus, the applied dose of ISO (1%) induced distinctive upregulation of NMDAR subunit (GRIN2A) along with the upregulation of postsynaptic density scaffold proteins (SHANK1, DLGAP1), and proteins of calcium/calmodulin cascade (RASGRF2, CaMKK1) [43,44]. In neocortex, the levels of these proteins (GRIN2A, SHANK1, DLGAP1, RASGRF2, and CaMKK1) were not changed in any of investigated anesthetics, except ISO-upregulated subunit of calcium/calmodulin kinase 2 (CaMK2G). GRIN2A and DLGAP1 were not quantified in MID, DEX, and DES and it was not possible to define hippocampal protein levels in DEX and DES. On the other hand, the upregulation of hippocampal SHANK1 was confirmed only in ISO as protein level upon DEX and DES remained unchanged. By contrast, the significant downregulation of hippocampal $\alpha 2/\delta 2$ -subunit of voltage-dependent calcium channel subunit induced by ISO was observed (Fig. 2A). Subsequently, we confirmed that the downregulation of CACNA2D2 was specific for hippocampus and only induced by ISO using immunoblotting (Fig. 3A). Further, the results revealed the downregulation of number of hippocampal proteins related to inhibitory signaling mediated by γ -aminobutyric acid (GABA) induced by ISO (NOS1, GAD1, ASS1, SLC32A1, CLDN11) [45–48] (Fig. 2A). Based on these proteomic results, we suggest ISO and possibly MID might enhance activity of NMDAR-CaM cascade and inhibit GABA signaling and presynaptic calcium release with potential to disrupt excitatory/inhibitory balance leading to neurodegenerative process especially in dose-dependent manner [49].

3.4. Impact of desflurane and dexmedetomidine to mitochondrial VDAC isoforms

Both, DES and DEX induced significant upregulation of neocortical and hippocampal voltage-dependent anion-selective channel protein isoforms (VDAC1, VDAC2, VDAC3), abundant mitochondrial membrane proteins, previously assessed as regulators of apoptosis [50] (Fig. 2B). The upregulation of VDAC localized in both neocortex and hippocampus was also confirmed using immunoblotting (Fig. 3A). VDAC is a key member of mitochondria-mediated apoptotic cascade as target of BCL-2 proteins and hexokinase (HK1). Complex VDAC with ADP/ATP translocases (ANT) is responsible for getting access of BAX to cytochrome C and membrane permeability [51]. However, none of anesthetics induced the significant dysregulation of other proteins quantified in this study and

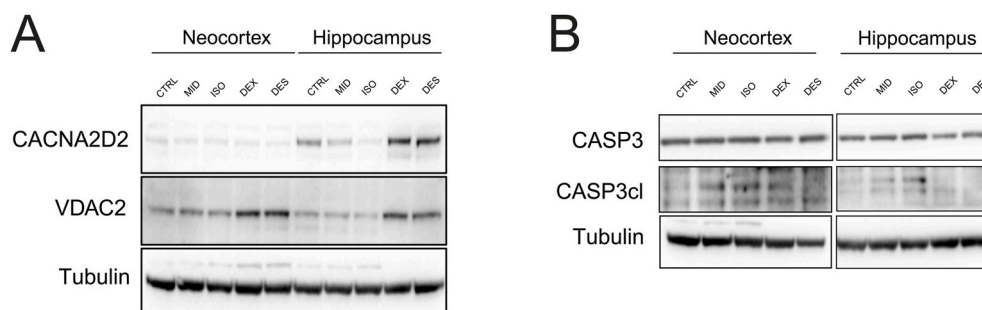


Fig. 3. Target quantification of selected proteins CACNA2D2, VDAC, and CASP3. (A) Protein levels of CACNA2D2 and VDAC2 determined in both brain tissues in control group and groups treated by anesthetics. Tubulin was used as a loading control. (B) Protein levels of CASP3 and its cleaved form determined in both brain tissues in control group and groups treated by anesthetics. Tubulin was used as a loading control.

related to apoptosis (BCLAF1, BCL2L13, AIFM1, ANT, PPID [52], ITPR1 and RYR2) in both neocortex and hippocampus (Fig. 2B). On the other hand, upregulation of neocortical HK1 induced by DEX and DES might suggest antiapoptotic regulatory HK1 interaction with VDACS [53–55]. In addition, the significant upregulation of neocortical GSTA4 might imply regulation of increased oxidative stress [56] in a response to DEX and DES anesthesia (Fig. 2B). To further evaluate the potential sensitivity of brain tissues to apoptosis induced by DEX and DES, we supplemented our study with targeted quantification of CASP3, major effector of calcium-dependent apoptosis [57]. However, changes of hippocampal CASP3 cleavage induced by DEX and DES were not observed using immunoblotting. On the contrary, we observed decreased level of cleaved CASP3 in case of MID and ISO in neocortex and hippocampus (Fig. 3B). We therefore suggest, that the doses of DEX and DES used in this study to simulate anesthesia, did not induce apoptosis through the upregulation of VDACS as itself, but the application of these anesthetic agents may increase the sensitivity of brain tissue to apoptotic stimuli [58] (e.g. hypoxia [59]).

4. Conclusions

In conclusion, comparative label-free LC-MS/MS study revealed 3603 neocortical and hippocampal proteins enabling to assess the impact of inhalational (ISO, DES) and intravenous (MID, DEX) anesthetics to brain centers for cognitive function (neocortex), learning and memory (hippocampus). *In vivo* study followed by mass spectrometry-based analysis proved mild global effect of investigated anesthetics to neocortical and hippocampal proteome, since the protein levels of less than 60 proteins were changed in case of investigated anesthetic drugs. On the other hand, dysregulation of these proteins revealed a distinct trend in ISO compared to DES as well as MID compared to DEX. Enhance activity of NMDAR-CaM signaling toward LTP along with downregulation of GABA signaling was observed especially upon ISO, whereas the upregulation of VDAC suggesting possible apoptotic activity was observed in DEX and DES. While ongoing activity of mitochondrial apoptotic pathway induced by DEX and DES was not confirmed, our data suggest the impact of those anesthetics to higher sensitivity to apoptotic stimuli. Collectively, presented data offer mechanistic insight into the effects routinely used anesthetics exert on brain and might lay the ground for future research aimed on mitigating their negative effects related to neurotoxicity and link to the development of POCD.

The limitation of this study is a relatively low number of biological replicates consisted from both male and female rats in each experimental group. However, the global proteomic study based on mass spectrometry are highly time-consuming procedure especially in case of wide-scale study, presented as comparative analysis of two brain structures upon application of 4 drugs. Therefore, we designed this work like rather “pilot” investigation to cover potential protein changes induced by selected anesthetics drugs in both genders. Label-free quantification is prone to missing values across samples, therefore we couldn't compare all significantly changed proteins among all experimental groups. On the other hand, proteomic results and conclusions achieved in LC-MS/MS were verified by immunoblotting of selected proteins in all anesthetics and both brain structures.

CRediT authorship contribution statement

David Astapenko: Writing – review & editing, Writing – original draft, Methodology, Conceptualization. **Marie Vajrychova:** Writing – review & editing, Writing – original draft, Visualization, Project administration, Methodology, Investigation, Data curation. **Ivo Fabrik:** Writing – review & editing, Writing – original draft, Validation. **Rudolf Kupcik:** Writing – review & editing, Writing – original draft, Data curation. **Kristyna Pimkova:** Writing – original draft, Methodology, Data curation. **Vojtech Tambor:** Writing – original draft, Methodology, Conceptualization. **Vera Radochova:** Methodology. **Vladimir Cerny:** Writing – review & editing, Writing – original draft, Supervision, Conceptualization.

Declaration of competing interest

The authors declare that they have no known competing financial interests or personal relationships that could have appeared to influence the work reported in this paper.

Acknowledgement

This work was supported by conceptual development of research organization (UHHK, 00179906), institutional support of Faculty of Medicine in Hradec Kralove, Charles University, and Next Generation EU, Programme EXCELES (LX22NPO5102). All authors wish to thank DVM Michal Pavlík from University of Defence (Brno, Czech Republic) for his valued help with *in vivo* experiment. The graphical abstract was prepared in BioRender (<https://biorender.com>).

Appendix A. Supplementary data

Supplementary data to this article can be found online at <https://doi.org/10.1016/j.heliyon.2024.e27638>.

References

- [1] D.B. Andropoulos, Effect of anesthesia on the developing brain: Infant and fetus, *Fetal Diagn. Ther.* 43 (2018) 1–11, <https://doi.org/10.1159/000475928>.
- [2] L. Vutskits, A. Davidson, Update on developmental anesthesia neurotoxicity, *Curr. Opin. Anaesthesiol.* 30 (2017) 337–342, <https://doi.org/10.1097/ACO.0000000000000461>.
- [3] N. Terrando, L.L. Eriksson, R.G. Eckenhoff, Perioperative neurotoxicity in the elderly: summary of the 4th International Workshop, *Anesth. Analg.* 120 (2015) 649–652, <https://doi.org/10.1213/ANE.0000000000000624>.
- [4] A. Luo, J. Yan, X. Tang, Y. Zhao, B. Zhou, S. Li, Postoperative cognitive dysfunction in the aged: the collision of neuroinflammation with perioperative neuroinflammation, *Inflammopharmacology* 27 (2019) 27–37, <https://doi.org/10.1007/s10787-018-00559-0>.
- [5] L. Wu, H. Zhao, H. Weng, D. Ma, Lasting effects of general anesthetics on the brain in the young and elderly: “mixed picture” of neurotoxicity, neuroprotection and cognitive impairment, *J. Anesth.* 33 (2019) 321–335, <https://doi.org/10.1007/s00540-019-02623-7>.
- [6] D. Yu, Y. Jiang, J. Gao, B. Liu, P. Chen, Repeated exposure to propofol potentiates neuroapoptosis and long-term behavioral deficits in neonatal rats, *Neurosci. Lett.* 534 (2013) 41–46, <https://doi.org/10.1016/j.neulet.2012.12.033>.
- [7] G. Stratmann, J.W. Sall, L.D.V. May, J.S. Bell, K.R. Magnusson, V. Rau, K.H. Visrodia, R.S. Alvi, B. Ku, M.T. Lee, et al., Isoflurane differentially affects neurogenesis and long-term neurocognitive function in 60-day-old and 7-day-old rats, *Anesthesiology* 110 (2009) 834–848, <https://doi.org/10.1097/ALN.0b013e31819c463d>.
- [8] W.E. Hoffman, E. Kochs, C. Werner, C. Thomas, R.F. Albrecht, Dexmedetomidine improves neurologic outcome from incomplete ischemia in the rat. Reversal by the alpha 2-adrenergic antagonist atipamezole, *Anesthesiology* 75 (1991) 328–332, <https://doi.org/10.1097/0000542-199108000-00022>.
- [9] C. Maier, G.K. Steinberg, G.H. Sun, G.T. Zhi, M. Maze, Neuroprotection by the alpha 2-adrenoreceptor agonist dexmedetomidine in a focal model of cerebral ischemia, *Anesthesiology* 79 (1993) 306–312, <https://doi.org/10.1097/0000542-199308000-00016>.
- [10] J.J. McAuliffe, A.W. Loepke, L. Miles, B. Joseph, E. Hughes, C.V. Vorhees, Desflurane, isoflurane, and sevoflurane provide limited neuroprotection against neonatal hypoxia-ischemia in a delayed preconditioning paradigm, *Anesthesiology* 111 (2009) 533–546, <https://doi.org/10.1097/ALN.0b013e3181b060d3>.
- [11] C.E. Griffin, A.M. Kaye, F.R. Bueno, A.D. Kaye, Benzodiazepine pharmacology and central nervous system-mediated effects, *Ochsner J.* 13 (2013) 214–223.
- [12] A. Shafer, Complications of sedation with midazolam in the intensive care unit and a comparison with other sedative regimens, *Crit. Care Med.* 26 (1998) 947–956, <https://doi.org/10.1097/00003246-199805000-00034>.
- [13] R.G. Greenberg, H. Wu, M. Laughon, E. Capparelli, S. Rowe, K.O. Zimmerman, P.B. Smith, M. Cohen-Wolkowicz, Population pharmacokinetics of dexmedetomidine in infants, *J. Clin. Pharmacol.* 57 (2017) 1174–1182, <https://doi.org/10.1002/jcph.904>.
- [14] J.A. Giovannitti, S.M. Thoms, J.J. Crawford, Alpha-2 adrenergic receptor agonists: a review of current clinical applications, *Anesth. Prog.* 62 (2015) 31–39, <https://doi.org/10.2344/0003-3006-62.1.31>.
- [15] M. McLaughlin, P.E. Marik, Dexmedetomidine and delirium in the ICU, *Ann. Transl. Med.* 4 (2016) 224, <https://doi.org/10.21037/atm.2016.05.44>.
- [16] M. Kaur, P.M. Singh, Current role of dexmedetomidine in clinical anesthesia and intensive care, *Anesth. Essays Res.* 5 (2011) 128–133, <https://doi.org/10.4103/0259-1162.94750>.
- [17] R.D. Sanders, J. Xu, Y. Shu, A. Januszewski, S. Halder, A. Fidalgo, P. Sun, M. Hossain, D. Ma, M. Maze, Dexmedetomidine attenuates isoflurane-induced neurocognitive impairment in neonatal rats, *Anesthesiology* 110 (2009) 1077–1085, <https://doi.org/10.1097/ALN.0b013e31819daedd>.
- [18] X. Su, Z.-T. Meng, X.-H. Wu, F. Cui, H.-L. Li, D.-X. Wang, X. Zhu, S.-N. Zhu, M. Maze, D. Ma, Dexmedetomidine for prevention of delirium in elderly patients after non-cardiac surgery: a randomised, double-blind, placebo-controlled trial, *Lancet* 388 (2016) 1893–1902, [https://doi.org/10.1016/S0140-6736\(16\)30580-3](https://doi.org/10.1016/S0140-6736(16)30580-3).
- [19] R.C. Terrell, The invention and development of enflurane, isoflurane, sevoflurane, and desflurane, *Anesthesiology* 108 (2008) 531–533, <https://doi.org/10.1097/ALN.0b013e31816499cc>.
- [20] W. Zhao, M. Zhang, J. Liu, P. Liang, R. Wang, H.C. Hemmings, C. Zhou, Isoflurane modulates hippocampal cornu ammonis pyramidal neuron excitability by inhibition of both transient and persistent sodium currents in mice, *Anesthesiology* 131 (2019) 94–104, <https://doi.org/10.1097/ALN.0000000000002753>.
- [21] D. Chai, H. Jiang, Q. Li, Isoflurane neurotoxicity involves activation of hypoxia inducible factor-1 α via intracellular calcium in neonatal rodents, *Brain Res.* 1653 (2016) 39–50, <https://doi.org/10.1016/j.brainres.2016.12.014>.
- [22] G. Tao, Q. Xue, Y. Luo, G. Li, Y. Xia, B. Yu, Isoflurane is more deleterious to developing brain than desflurane: the role of the Akt/GSK3 β signaling pathway, *BioMed Res. Int.* 2016 (2016) 7919640, <https://doi.org/10.1155/2016/7919640>.
- [23] M. Perouansky, H.C. Hemmings, Neurotoxicity of general anesthetics: cause for concern? *Anesthesiology* 111 (2009) 1365–1371, <https://doi.org/10.1097/ALN.0b013e3181bf1d61>.
- [24] D. Yu, L. Li, W. Yuan, Neonatal anesthetic neurotoxicity: insight into the molecular mechanisms of long-term neurocognitive deficits, *Biomed. Pharmacother.* 87 (2017) 196–199, <https://doi.org/10.1016/j.biopha.2016.12.062>.
- [25] E.D. Kharasch, D.C. Hankins, K.E. Thummel, Human kidney methoxyflurane and sevoflurane metabolism. Intrarenal fluoride production as a possible mechanism of methoxyflurane nephrotoxicity, *Anesthesiology* 82 (1995) 689–699, <https://doi.org/10.1097/0000542-199503000-00011>.
- [26] N. Topf, A. Jenkins, N. Baron, N.L. Harrison, Effects of isoflurane on gamma-aminobutyric acid type A receptors activated by full and partial agonists, *Anesthesiology* 98 (2003) 306–311, <https://doi.org/10.1097/0000542-200302000-00007>.
- [27] K. Nishikawa, N.L. Harrison, The actions of sevoflurane and desflurane on the gamma-aminobutyric acid receptor type A: effects of TM2 mutations in the alpha and beta subunits, *Anesthesiology* 99 (2003) 678–684, <https://doi.org/10.1097/0000542-200309000-00024>.
- [28] R.M. Jones, Desflurane and sevoflurane: inhalation anaesthetics for this decade? *Br. J. Anaesth.* 65 (1990) 527–536, <https://doi.org/10.1093/bja/65.4.527>.
- [29] B. Zhang, M. Tian, Y. Zhen, Y. Yue, J. Sherman, H. Zheng, S. Li, R.E. Tanzi, E.R. Marcantonio, Z. Xie, The effects of isoflurane and desflurane on cognitive function in humans, *Anesth. Analg.* 114 (2012) 410–415, <https://doi.org/10.1213/ANE.0b013e31823b2602>.
- [30] D. Rörtgen, J. Kloos, M. Fries, O. Grottko, S. Rex, R. Rossaint, M. Coburn, Comparison of early cognitive function and recovery after desflurane or sevoflurane anaesthesia in the elderly: a double-blinded randomized controlled trial, *Br. J. Anaesth.* 104 (2010) 167–174, <https://doi.org/10.1093/bja/aep369>.
- [31] J.R. Sned, Thiopental to desflurane - an anaesthetic journey. Where are we going next? *Br. J. Anaesth.* 119 (2017) <https://doi.org/10.1093/bja/aex328> i44–i52.
- [32] D. Miller, S.R. Lewis, M.W. Pritchard, O.J. Schofield-Robinson, C.L. Shelton, P. Alderson, A.F. Smith, Intravenous versus inhalational maintenance of anaesthesia for postoperative cognitive outcomes in elderly people undergoing non-cardiac surgery, *Cochrane Database Syst. Rev.* 8 (2018) CD012317, <https://doi.org/10.1002/14651858.CD012317.pub2>.
- [33] L. Ping, S.R. Kundinger, D.M. Duong, L. Yin, M. Gearing, J.J. Lah, A.I. Levey, N.T. Seyfried, Global quantitative analysis of the human brain proteome and phosphoproteome in Alzheimer’s disease, *Sci. Data* 7 (2020) 315, <https://doi.org/10.1038/s41597-020-00650-8>.
- [34] Y. Perez-Riverol, A. Csordas, J. Bai, M. Bernal-Llinares, S. Hewapathirana, D.J. Kundu, A. Inuganti, J. Griss, G. Mayer, M. Eisenacher, et al., The PRIDE database and related tools and resources in 2019: improving support for quantification data, *Nucleic Acids Res.* 47 (2019) D442–D450, <https://doi.org/10.1093/nar/gky1106>.
- [35] J. Cox, M. Mann, MaxQuant enables high peptide identification rates, individualized p.p.b.-range mass accuracies and proteome-wide protein quantification, *Nat. Biotechnol.* 26 (2008) 1367–1372, <https://doi.org/10.1038/nbt.1511>.
- [36] J. Cox, M.Y. Hein, C.A. Luber, I. Paron, N. Nagaraj, M. Mann, Accurate proteome-wide label-free quantification by delayed normalization and maximal peptide ratio extraction, termed MaxLFQ, *Mol. Cell. Proteomics* 13 (2014) 2513–2526, <https://doi.org/10.1074/mcp.M113.031591>.
- [37] S. Tyanova, T. Temu, P. Sinitcyn, A. Carlson, M.Y. Hein, T. Geiger, M. Mann, J. Cox, The Perseus computational platform for comprehensive analysis of (prote) omics data, *Nat. Methods* 13 (2016) 731–740, <https://doi.org/10.1038/nmeth.3901>.
- [38] H.D.I. Abarbanel, R. Huerta, M.I. Rabinovich, Dynamical model of long-term synaptic plasticity, *Proc. Natl. Acad. Sci. U.S.A.* 99 (2002) 10132–10137, <https://doi.org/10.1073/pnas.132651299>.
- [39] P.J. Magistretti, I. Allaman, A cellular perspective on brain energy metabolism and functional imaging, *Neuron* 86 (2015) 883–901, <https://doi.org/10.1016/j.neuron.2015.03.035>.

- [40] H. Wei, B. Kang, W. Wei, G. Liang, Q.C. Meng, Y. Li, R.G. Eckenhoff, Isoflurane and sevoflurane affect cell survival and BCL-2/BAX ratio differently, *Brain Res.* 1037 (2005) 139–147, <https://doi.org/10.1016/j.brainres.2005.01.009>.
- [41] H. Wei, G. Liang, H. Yang, Q. Wang, B. Hawkins, M. Madesh, S. Wang, R.G. Eckenhoff, The common inhalational anesthetic isoflurane induces apoptosis via activation of inositol 1,4,5-trisphosphate receptors, *Anesthesiology* 108 (2008) 251–260, <https://doi.org/10.1097/01.anes.0000299435.59242.0e>.
- [42] G. Liang, Q. Wang, Y. Li, B. Kang, M.F. Eckenhoff, R.G. Eckenhoff, H. Wei, A presenilin-1 mutation renders neurons vulnerable to isoflurane toxicity, *Anesth. Analg.* 106 (2008) 492–500, table of contents. 10.1213/ane.0b013e3181605b71.
- [43] B. Schwechter, C. Rosenmund, K.F. Tolias, RasGRF2 Rac-GEF activity couples NMDA receptor calcium flux to enhanced synaptic transmission, *Proc. Natl. Acad. Sci. U.S.A.* 110 (2013) 14462–14467, <https://doi.org/10.1073/pnas.1304340110>.
- [44] H. Ma, R.D. Groth, S.M. Cohen, J.F. Emery, B. Li, E. Hoedt, G. Zhang, T.A. Neubert, R.W. Tsien, γ CaMKII shuttles Ca^{2+} /CaM to the nucleus to trigger CREB phosphorylation and gene expression, *Cell* 159 (2014) 281–294, <https://doi.org/10.1016/j.cell.2014.09.019>.
- [45] G. Fenalti, R.H.P. Law, A.M. Buckle, C. Langendorf, K. Tuck, C.J. Rosado, N.G. Faux, K. Mahmood, C.S. Hampe, J.P. Banga, et al., GABA production by glutamic acid decarboxylase is regulated by a dynamic catalytic loop, *Nat. Struct. Mol. Biol.* 14 (2007) 280–286, <https://doi.org/10.1038/nsmb1228>.
- [46] C.D.S. Barros, J.B. Livramento, M.G. Moura, E.M.S. Higa, C.T. Moraes, C.H. Tengan, L-arginine reduces nitro-oxidative stress in cultured cells with mitochondrial deficiency, *Nutrients* 13 (2021) 534, <https://doi.org/10.3390/nu13020534>.
- [47] B. Gasnier, The SLC32 transporter, a key protein for the synaptic release of inhibitory amino acids, *Pflügers Arch* 447 (2004) 756–759, <https://doi.org/10.1007/s00424-003-1091-2>.
- [48] K.J. Maheras, M. Peppi, F. Ghodoussi, M.P. Galloway, S.A. Perrine, A. Gow, Absence of claudin 11 in CNS myelin perturbs behavior and neurotransmitter levels in mice, *Sci. Rep.* 8 (2018) 3798, <https://doi.org/10.1038/s41598-018-22047-9>.
- [49] V. Jevtic-Todorovic, R.E. Hartman, Y. Izumi, N.D. Benschoff, K. Dikranian, C.F. Zorumski, J.W. Olney, D.F. Wozniak, Early exposure to common anesthetic agents causes widespread neurodegeneration in the developing rat brain and persistent learning deficits, *J. Neurosci.* 23 (2003) 876–882, <https://doi.org/10.1523/JNEUROSCI.23-03-00876.2003>.
- [50] S. Shimizu, M. Narita, Y. Tsujimoto, Bcl-2 family proteins regulate the release of apoptogenic cytochrome c by the mitochondrial channel VDAC, *Nature* 399 (1999) 483–487, <https://doi.org/10.1038/20959>.
- [51] M.Y. Vyssokikh, D. Brdiczka, The function of complexes between the outer mitochondrial membrane pore (VDAC) and the adenine nucleotide translocase in regulation of energy metabolism and apoptosis, *Acta Biochim. Pol.* 50 (2003) 389–404.
- [52] M. Crompton, S. Virji, J.M. Ward, Cyclophilin-D binds strongly to complexes of the voltage-dependent anion channel and the adenine nucleotide translocase to form the permeability transition pore, *Eur. J. Biochem.* 258 (1998) 729–735, <https://doi.org/10.1046/j.1432-1327.1998.2580729.x>.
- [53] H. Zaid, S. Abu-Hamad, A. Israelson, I. Nathan, V. Shoshan-Barmatz, The voltage-dependent anion channel-1 modulates apoptotic cell death, *Cell Death Differ.* 12 (2005) 751–760, <https://doi.org/10.1038/sj.cdd.4401599>.
- [54] J. Lauterwasser, F. Fimm-Todt, A. Oelgeklaus, A. Schreiner, K. Funk, H. Falquez-Medina, R. Klesse, G. Jahreis, R.M. Zerbe, K. O'Neill, et al., Hexokinases inhibit death receptor-dependent apoptosis on the mitochondria, *Proc. Natl. Acad. Sci. U.S.A.* 118 (2021) e2021175118, <https://doi.org/10.1073/pnas.2021175118>.
- [55] A. Schoeniger, P. Wolf, F. Edlich, How do hexokinases inhibit receptor-mediated apoptosis? *Biology* 11 (2022) 412, <https://doi.org/10.3390/biology11030412>.
- [56] S. Goto, M. Kawakatsu, S.-I. Izumi, Y. Urata, K. Kageyama, Y. Ihara, T. Koji, T. Kondo, Glutathione S-transferase pi localizes in mitochondria and protects against oxidative stress, *Free Radic. Biol. Med.* 46 (2009) 1392–1403, <https://doi.org/10.1016/j.freeradbiomed.2009.02.025>.
- [57] S. Krajewski, M. Krajewska, L.M. Ellerby, K. Welsh, Z. Xie, Q.L. Deveraux, G.S. Salvesen, D.E. Bredesen, R.E. Rosenthal, G. Fiskum, et al., Release of caspase-9 from mitochondria during neuronal apoptosis and cerebral ischemia, *Proc. Natl. Acad. Sci. U.S.A.* 96 (1999) 5752–5757, <https://doi.org/10.1073/pnas.96.10.5752>.
- [58] V. Shoshan-Barmatz, S. De, A. Meir, The mitochondrial voltage-dependent anion channel 1, Ca^{2+} transport, apoptosis, and their regulation, *Front. Oncol.* 7 (2017) 60, <https://doi.org/10.3389/fonc.2017.00060>.
- [59] X. Wang, J. Li, D. Wu, X. Bu, Y. Qiao, Hypoxia promotes apoptosis of neuronal cells through hypoxia-inducible factor-1 α -microRNA-204-B-cell lymphoma-2 pathway, *Exp Biol Med (Maywood)* 241 (2016) 177–183, <https://doi.org/10.1177/1535370215600548>.